

See discussions, stats, and author profiles for this publication at: <https://www.researchgate.net/publication/241942236>

High coverages and subsurface penetration of oxygen on Ru(001)

ARTICLE · JANUARY 1991

CITATION

1

READS

8

2 AUTHORS, INCLUDING:



[Jan Hrbek](#)

Brookhaven National Laboratory

214 PUBLICATIONS **6,049** CITATIONS

SEE PROFILE

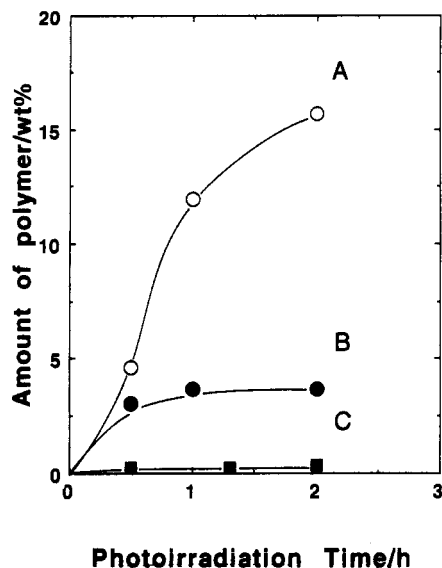


Figure 6. Relation between the amount of the polymer on the particles and photoirradiation time in the case where various siloxanes were used as the reactants: A, reactant = TMCTS; B, reactant = OMCTS; C, reactant = PDMS (MW = 2500).

to be noted that the degree of the coloration increased as the cutoff wavelength of the filter decreases.

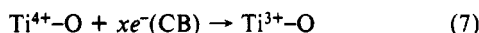


Figure 6 shows the reactivities of OMCTS and PDMS (MW = 2500) compared with that of TMCTS. The polymerization

of OMCTS which is also a cyclotetrasiloxane takes place similarly to TMCTS, whereas the amount of linear PDMS ranging from 0.20 to 0.36 wt % is of the order of the adsorption on SiO_2 (<0.28 wt %).¹⁷ It is noteworthy that this quantity is 5.7 ± 1.5 times less than that of TMCTS reacted in the dark.

The rate of the polymerization of OMCTS is significantly smaller than that of TMCTS. Since additional methyl groups of OMCTS reduce the ionization potential,¹¹ the electron transfer from OMCTS to the hole in the VB of TiO_2 would occur in a similar manner as the case of TMCTS (eq 3). If the rate-determining step of the polymerization is presumed to be the attack on TMCTS (or OMCTS) molecules by TMCTS^+ (or OMCTS^+), the smaller rate for OMCTS can be explained in terms of the steric hindrance due to the four additional methyl groups of OMCTS. These facts above are consistent with the ring-opening polymerization mechanism of TMCTS driven by the oxidation due to the hole in the VB of TiO_2 particles (eq 4).

This is, to our knowledge, the first report on the photoinduced polymerization directly caused by the electronically excited semiconductor particles.

From an aspect of application, this photoinduced polymerization provides a novel method for surface modification of fine semiconductor particles, which is prerequisite for its high functionalization.

Acknowledgment. We wish to express our gratitude to M. Hirata and Y. Saito for their generous support of this research.

(17) Tada, H.; Saito, Y.; Hirata, M.; Hyodo, M.; Kawahara, H. *Jpn. Colour Mater.* **1991**, *64*, 12.

High Coverages and Subsurface Penetration of Oxygen on Ru(001)

Igor J. Malik[†] and Jan Hrbek^{*}

Department of Chemistry, Brookhaven National Laboratory, Upton, New York 11973
(Received: August 8, 1991)

Interaction of NO_2 , an effective source of atomic oxygen, with a Ru(001) single crystal face was studied at substrate temperatures 400–800 K. We present thermal desorption spectroscopy data indicating that up to 40 oxygen monolayers can be accommodated within the surface and subsurface regions. Once oxygen penetrates below the surface, fragments containing Ru atoms (RuO_x , $x = 0\text{--}3$) are detected during desorption and O_2 desorbs with near-zero-order kinetics. We briefly discuss these experimental results in terms of a model for subsurface penetration of oxygen on transition metals.

Oxygen is known to adsorb dissociatively on the close-packed Ru(001) surface and to form ordered overlayer structures at coverages $\theta = 0.25$ and 0.5^{1-3} with the oxygen adatoms occupying tetrahedral (3-fold hcp) sites.⁴ $\theta = 0.5$ corresponds to a saturation coverage under "UHV conditions".^{2,3} TDS (thermal desorption spectroscopy) and AES (Auger electron spectroscopy) results^{2,3} indicate that diffusion of the O adatoms into the Ru bulk is a competing channel for removal of oxygen from the surface while heating the substrate. The bulk diffusion rate seems to be significant only at temperatures^{3,5,6} above ≈ 1150 K, although one study claims that this channel is open already at 400 K.⁷ In our previous studies of oxygen coadsorption with Au on Ru(001),^{5,6} we estimated that heating the Ru(001) surface with $\theta = 0.5$ results in desorption of $\approx 50\%$ of the total amount of oxygen and diffusion into the Ru bulk of the other $\approx 50\%$.

NO_2 has been used for achieving higher oxygen coverages than possible with O_2 on Pt(111),⁸ Pd(111),⁹ and GaAs.¹⁰ For the

metal surfaces, this observation was explained⁹ by a high (≈ 1 for $T \geq 300$ K) dissociative sticking coefficient, S_d , for the process $\text{NO}_2 \rightarrow \text{NO}_a + \text{O}_a$ (subscript a means adsorbed). S_d for NO_2 is essentially coverage independent; this contrasts with S_d for the process $\text{O}_2 \rightarrow 2\text{O}_a$ for which S_d drops from ≈ 0.37 for a clean surface to a negligible value for $\theta = 0.5$.² Keeping the substrate above NO-desorption temperature (NO desorption from Ru(001)

(1) Rahman, T. S.; Anton, A. B.; Avery, N. R.; Weinberg, W. H. *Phys. Rev. Lett.* **1983**, *51*, 1979.

(2) Madey, T. E.; Engelhardt, H. A.; Menzel, D. *Surf. Sci.* **1975**, *48*, 304.

(3) Surnev, L.; Rangelov, G.; Bliznakov, G. *Surf. Sci.* **1985**, *159*, 299.

(4) Pfnür, H.; Held, G.; Lindroos, M.; Menzel, D. *Surf. Sci.* **1989**, *220*, 43.

(5) Malik, I. J.; Hrbek, J. *J. Phys. Chem.* **1991**, *95*, 2466.

(6) Malik, I. J.; Hrbek, J. *J. Vac. Sci. Technol. A* **1991**, *9*, 1806.

(7) Praline, G.; Koel, B. E.; Lee, H.-I.; White, J. M. *Appl. Surf. Sci.* **1980**, *5*, 296.

(8) Parker, D. H.; Bartram, M. E.; Koel, B. E. *Surf. Sci.* **1989**, *217*, 489.

(9) Banse, B. A.; Koel, B. E. *Surf. Sci.* **1990**, *232*, 275.

(10) vom Felde, A.; Kern, K.; Higashi, G. S.; Chabal, Y. J.; Christman, S. B.; Bahr, C. C.; Cardillo, M. *J. Phys. Rev. B* **1990**, *42*, 5240.

[†] Present address: MEMC Electronic Materials, Inc., 501 Pearl Drive, P.O. Box 8, St. Peters, MO 63376.

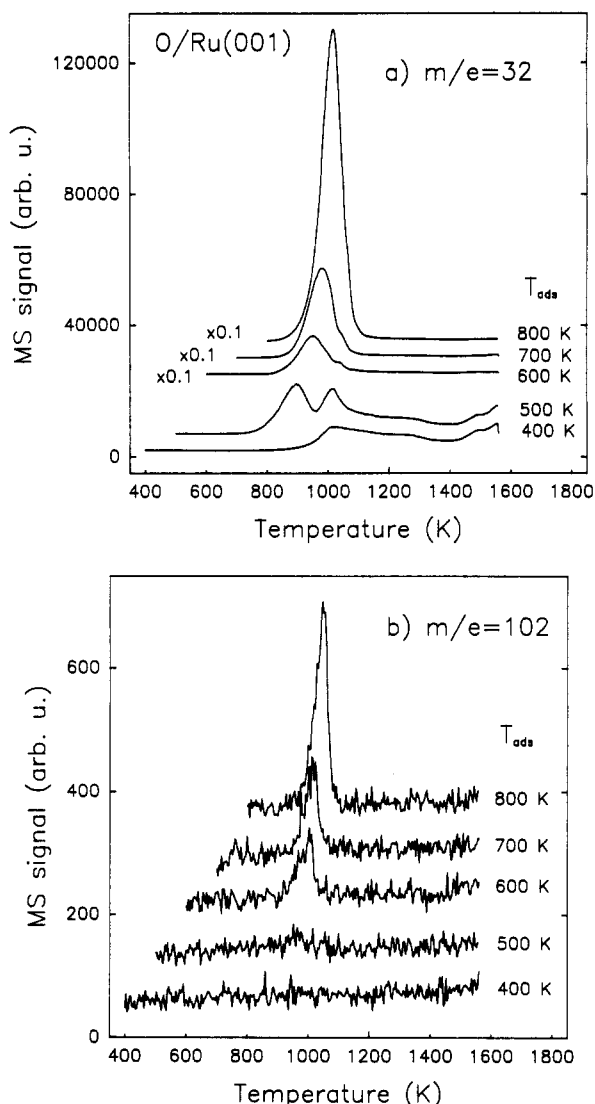


Figure 1. O₂ (a) and ¹⁰²Ru (b) TDS traces after exposing a Ru(001) substrate to "450 langmuirs" of NO₂ at various substrate temperatures between 400 and 800 K. The integrated TDS areas correspond to the following coverages for O₂ (¹⁰²Ru): 400 K, $\theta = 1.4$ ($R_{\text{loss}} < 0.1$); 500 K, 2.8 (< 0.1); 600 K, 7.5 (0.8); 700 K, 14 (0.8); 800 K, 40 (1.7).

is completed at ≈ 500 K¹¹) is clearly important for achieving high oxygen coverages from exposures to NO₂.

The experiments were performed in an ion-pumped UHV system with a base pressure of 1×10^{-10} Torr.⁵ The Ru(001) crystal was mounted and resistively heated by two W wires spot welded to the side edges of the crystal; it was cleaned by sputtering followed by several cycles of oxygen adsorption-desorption. The crystal can be heated to 1560 K and cooled to 80 K by liquid nitrogen. NO₂ (Matheson)¹² was introduced into the chamber through a glass capillary array doser facing the crystal with ≈ 5 -mm distance between them. We do not know the exact exposures of the crystal to NO₂ (the doser is not calibrated in terms of molecular flux); we therefore present exposures in langmuirs (1 langmuir = 10^{-6} Torr-s) in quotation marks referring to the exposure time multiplied by the background pressure in the chamber (the actual exposures are higher). The TDS data were collected with a differentially pumped QMS (quadrupole mass spectrometer) equipped with a stainless steel skimmer with a ≈ 3 -mm opening facing the crystal positioned at a distance of ≈ 3

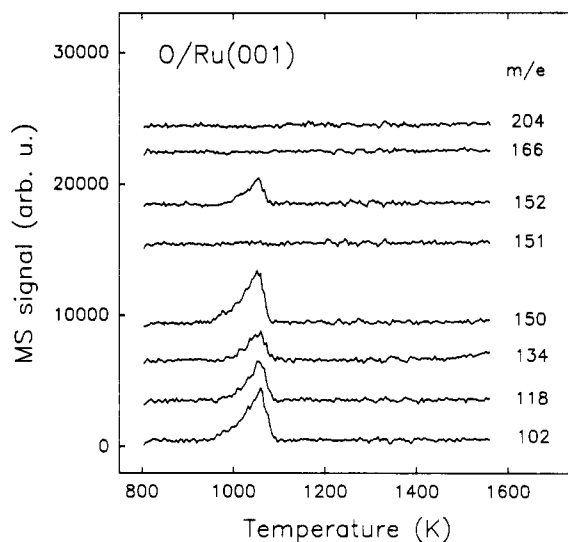


Figure 2. TDS traces of various ions after a "450 langmuirs" NO₂ exposure with the Ru(001) substrate at 800 K: ¹⁰²Ru⁺ ($m/e = 102$), ¹⁰²RuO⁺ (118), ¹⁰²RuO₂⁺ (134), ¹⁰²RuO₃⁺ (150), a dummy signal (151), ¹⁰⁴RuO₃⁺ (152), ¹⁰²RuO₄⁺ (166), and ¹⁰²Ru₂⁺ (204).

mm from the skimmer. The QMS is interfaced with a personal computer for multiplexing; the linear heating rate during collection of TDS traces was 2 K/s.

Figure 1 shows TDS traces of the O₂ ($m/e = 32$) and the most abundant isotope of Ru ($m/e = 102$) signals from the Ru(001) surface exposed to "450 langmuirs" of NO₂ at surface temperatures varying between 400 and 800 K. We also obtained a series of TDS traces after different NO₂ and O₂ exposures with the Ru crystal at 600 K—the main features of these traces are the same as of those shown in Figure 1; the maximum oxygen coverage from dosing O₂ at 600 K was $\theta = 1.4$.¹³

The integration of the 400 K O₂ trace in Figure 1 gives $\theta \approx 1.4$ assuming a saturation coverage under UHV condition $\theta = 0.5$ and $\approx 50\%$ oxygen loss due to the bulk diffusion⁵. No Ru desorption is detected under these conditions. A Ru signal is first observable after a 600 K exposure when the O₂ integrated area indicates $\theta \approx 7.5$. The 800 K exposure resulted in $\theta \approx 40$, and the integrated area of the Ru signal indicates a removal of ≈ 2 monolayers of Ru ($R_{\text{loss}} \approx 1.7$). This value of R_{loss} was obtained from a calibration with an adsorbed Ag monolayer (the first and additional adsorbed layers of Ag can be clearly distinguished in TDS¹⁴) while taking into account the natural abundances of the Ag and Ru isotopes. We assumed that Ru is detected in the form of four different ions RuO_x⁺ ($x = 0-3$) with an intensity distribution between these four ions shown in Figure 2: 32% $x = 0$, 24% $x = 1$, 16% $x = 2$, and 28% $x = 3$. Additional simplifying assumptions in the estimation of the amount of desorbed Ru were that the ionization efficiencies (in the QMS ionizer) and angular distributions of the desorbing species are the same for RuO_x and Ag.

Figure 2 displays TDS traces of various ions after a "450 langmuirs" NO₂ exposure at 800 K. The ions shown are as follows: ¹⁰²Ru⁺ ($m/e = 102$), ¹⁰²RuO⁺ ($m/e = 118$), ¹⁰²RuO₂⁺ ($m/e = 134$), ¹⁰²RuO₃⁺ ($m/e = 150$), a dummy signal ($m/e = 151$); there is no ¹⁰³Ru natural isotope, ¹⁰⁴RuO₃⁺ ($m/e = 152$), ¹⁰²RuO₄⁺ ($m/e = 166$), and ¹⁰²Ru₂⁺ ($m/e = 204$). Ru leaving the surface can be clearly detected as RuO_x⁺, x being 0-3. We did not detect any RuO₄⁺ or Ru₂⁺ signals. The intensity ratio of $m/e = 150$ to $m/e = 152$ is in good agreement with that of the natural abundance of ¹⁰²Ru (31.61%) to ¹⁰⁴Ru (18.58%).

The oxygen uptake resulting in $\theta = 40$ (which still does not represent saturation) is an unprecedented result requiring a more detailed discussion. There are several possibilities to explain such

(11) Hayden, B. E.; Kretzschmar, K.; Bradshaw, A. M. *Surf. Sci.* **1983**, *125*, 366.

(12) We would like to issue a word of warning about the aggressiveness of NO₂: Cu gaskets that were in contact with the gas were covered with a black layer of copper oxide, and the copper-sapphire seals of leak valves used were quickly (\approx several days) losing their sealing ability.

(13) Malik, I. J.; Hrbek, J. In preparation.

(14) Niemantsverdriet, J. W.; Dolle, P.; Markert, K.; Wandelt, K. *J. Vac. Sci. Technol. A* **1987**, *5*, 875.

a high coverage. The most obvious one, growth of a molecular oxygen multilayer, can be rejected because of experimental temperatures involved and results from several surface probes. Also, there is no sign of Ru metal oxidation. Experimentally, we find no evidence for the formation of molecular oxygen, surface dioxygen species, or ruthenium oxides in our valence band, core level photoemission, and Auger spectra.¹³ The results of all three techniques provided a proof for the presence of chemisorbed atomic oxygen. Faceting as another explanation for high oxygen coverage is also unlikely; facets are inclined crystal planes closely related to the original surface and are often induced by adsorption at submonolayer coverages. To account for the high oxygen coverage measured, facets with very steep sides would have to be invoked.

We thus dismiss faceting as well as bulk oxidation and molecular adsorption and propose that oxygen penetrates into the subsurface region. Two experimental results found in the TDS data support this proposal: The first one is the appearance of the RuO_x^+ signals (Figures 1b, 2) seen in TDS only after surface coverage $\theta > 2$ was reached. Another is the advent of a low-temperature O_2 TDS peak (at 900 K for the 500 K exposure, Figure 1a) and its behavior. The low-temperature peak grows with the temperature of exposure (i.e., θ) and already for the 600 K exposure conceals the high-temperature peak. The low-temperature peak does not saturate and shows approximately zero-order behavior. Desorption from surface/subsurface states is known to lead to the near-zero-order kinetics.¹⁵ An Arrhenius plot for the 800 K exposure (based on the assumption that the desorption is zero-order) yields 211 kJ/mol for E_A , the activation energy of desorption for O_2 . This value is considerably lower than E_A values reported for $\theta = 0.5$: 335 (ref 2) and 315 (ref 3) kJ/mol. The nature of the irreversible oxygen diffusion into the Ru bulk discussed for oxygen coverages $\theta \leq 0.5$ (with the onset at $\approx 1150 \text{ K}$)²⁻⁶ is markedly different from the oxygen subsurface penetration at temperatures as low as 600 K.

We note that a coverage of at least two monolayers of oxygen ($\theta > \approx 2$) is required before oxygen commences the subsurface penetration. On the surface covered with a compressed oxygen layer at e.g. $\theta = 3$, the O-O bond distance is 1.56 Å, close to that found in the peroxide ion, O_2^{2-} , i.e. 1.49 Å.¹⁶ With no experimental proof for dioxygen species formation,¹³ the upper limit of surface saturation can be put at $\theta = 3$, and we expect that the strong repulsion between oxygen adatoms will lower the heat of adsorption significantly. It is plausible that the higher-temperature O_2 peak (at 1020 K for 500 K exposure) originates from the recombination of surface O atoms in such a compressed layer.

The oxygen subsurface penetration can be explained, at least qualitatively, by a model dealing with oxygen chemisorption and subsurface incorporation on transition-metal surfaces.¹⁷ The main

idea of this model is that the lattice distortion energy for a single subsurface oxygen atom is much larger than that, per oxygen atom, of a complete oxygen underlayer. Therefore, once the first oxygen atom penetrates below the surface, it acts as a "seed" of an oxygen underlayer. The results reported here suggest that for the O/Ru(001) system with $\theta = 40$ the penetration occurs into a region at least ≈ 10 Ru layers below the surface. This is compatible with the concept of a subsurface selvedge, a region several monolayers thick with properties intermediate between surface and bulk,¹⁸ able to take up a finite amount of adsorbate. The presence of an adsorbate might lower the cohesive energy of the selvedge substrate atoms to such a degree that they leave the surface together with the adsorbate.

The subsurface penetration mechanism is probably related to the surface phonon softening (increase in the atomic displacement) observed by inelastic He scattering on the close-packed Pt(111) surface upon oxygen adsorption.¹⁹ The mode that experiences this softening most dramatically corresponds to a simultaneous motion of neighboring metal atoms resulting in opening and closing of the 3-fold hollow sites. It is feasible to expect this mode to play a crucial role in the oxygen subsurface penetration with the oxygen atoms penetrating preferably through the fcc sites.

Finally, we would like to comment on the desorption fragments containing Ru, RuO_x^+ . A related observation of substrate atoms desorbing together with the adsorbate has been reported recently for the H/Al(111) system;²⁰ the presence of aluminum hydride in the surface region was suggested. While the detection of the RuO_3^+ signal in our experiments opens the possibility of RuO_3 presence on the surface prior to desorption, photoemission data offer no support for it.¹³ A more probable explanation is the formation of RuO_3 , a species observed in the gas phase,²¹ during the temperature ramp.

In this paper, we report TDS results obtained after exposures of a Ru(001) surface at temperatures 400–800 K to NO_2 . The integrated areas of the O_2 -desorption traces correspond to coverages up to $\theta \approx 40$ with respect to Ru surface atom density. The detection of RuO_x ($x = 0-3$) TDS signals and near-zero-order desorption of O_2 suggest the subsurface oxygen penetration; the minimum oxygen coverage for the onset of this process is $\theta \approx 2$. Photoemission results¹³ show no indication of oxide formation even at the highest oxygen coverages achieved.

Acknowledgment. This research was carried out at Brookhaven National Laboratory under Contract No. DE-AC02-76CH00016 with the U.S. Department of Energy and supported by its Division of Chemical Sciences, Office of Basic Energy Sciences.

(15) Behm, R. J.; Penka, V.; Cattania, M.-G.; Christmann, K.; Ertl, G. *J. Chem. Phys.* **1983**, *78*, 7486. Gdowski, G. E.; Felner, T. R.; Stulen, R. H. *Surface Sci.* **1987**, *181*, L147.

(16) Cotton, F. A.; Wilkinson, G. *Advanced Inorganic Chemistry*, 4th ed.; J. Wiley & Sons: New York, 1980; p 499.

(17) Chakraborty, B.; Holloway, S.; Nørskov, J. K. *Surf. Sci.* **1985**, *152/153*, 660.

(18) Daitzschmann, C.; Aharoni, C.; Ungarish, M. *Surf. Sci.* **1991**, *244*, 362.

(19) Neuhaus, D.; Joo, F.; Feuerbacher, B. *Phys. Rev. Lett.* **1987**, *58*, 694.

(20) Hara, M.; Domen, K.; Onishi, T.; Nozoye, H. *J. Phys. Chem.* **1991**, *95*, 6.

(21) Rard, J. A. *Chem. Rev.* **1985**, *85*, 1.